Active Vibration Control of Composite Shell Structure using Modal Sensor/Actuator System

Seung Jo Kim*, Joon Seok Hwang and Jiwon Mok*****
School of Mechanical and Aerospace Engineering,
Seoul National University, Korea 151-742

Abstract

The active vibration control of composite shell structure has been performed with the optimized sensor/actuator system. For the design of sensor/actuator system, a method based on finite element technique is developed. The nine-node Mindlin shell element has been used for modeling the integrated system of laminated composite shell with PVDF sensor/actuator. The distributed selective modal sensor/actuator system is established to prevent the effect of spillover. Electrode patterns and lamination angles of sensor/actuator are optimized using genetic algorithm. Continuous electrode patterns are discretized according to finite element mesh, and orientation angle is encoded into discrete values using binary string. Sensor is designed to minimize the observation spillover, and actuator is designed to minimize the system energy of the control modes under a given initial condition. Modal sensor/actuator for the first and the second mode vibration control of singly curved cantilevered composite shell structure are designed with the method developed on the finite element method and optimization. For verification, the experimental test of the active vibration control is performed for the composite shell structure. Discrete LQG method is used as a control law.

Key Word : Composite shell structure, Active vibration control, Sensor/Actuator System, Finite element method, Genetic Algorithm

Introduction

Throughout the history of aircraft manufacturing, the structures get thinner and the material becomes lighter. Thus the composite material gradually expands its territory, because it is light, moreover, strong and stiff. The skins of aircraft are the most critical parts, because they are in the figure of thin plate or thin shell. To ensure the dynamic stability in these structures, it is extremely important to control the vibration.

In the active vibration control, there needs sensor, actuator and controller to control the vibration of the structure. Among many kinds of smart materials, piezoelectric material is largely used in the vibration or acoustic control. Lead-zirconate-titanate (PZT) ceramics and polyvinylidene fluoride (PVDF) film are the most popular ones. While PZT has been generally used as an actuator for its considerable actuating force, PVDF film is employed as material of distributed sensor and actuator both, because it is flexible, lightweight and easy to shape the electrode pattern.

Due to the computational limitation, it is not able to consider all the modes of a continuum

* Professor, Flight Vehicle Research Center, corresponding author
E-mail : sjkim@snu.ac.kr Tel : 02-880-7388 Fax : 02-887-2662
** Research assistant, currently works for the Korean Intellectual Property Office
*** Research assistant, currently Ph.D candiate at University of Michigan Ann Arbor

structure. Thus only a few modes which critically affect the characteristics of vibration are selectively concerned in the vibration control. The residual modes, which are not considered in the controller design, may cause the well-known phenomenon of spillover[1]. The observation and control spillover from residual modes may provoke instability in the closed loop system. To avoid this phenomenon, the residual modes must be cut off. The electrical filter, which is commonly used to cut off residual modes, may induce the phase distortion near cutoff frequency. For the modal transducer[2] is able to sense or actuate specific modes directly, it can effectively prevent the adverse effect of spillover without inducing phase change. The modal transducer is significantly useful in the case that the adjacent modes are close, which appears frequently in composite structures. Kim et al[3] had shown the good performance of the distributed modal transducer in the vibration control of composite plate.

Although a lot of research has been focused on the active vibration control of the structures using piezoelectric material, the research on active vibration control of shell structure is relatively rare. Tzou et al4 investigated on the static and dynamic behaviors of circular shallow spherical shells with geometric nonlinear deformation. Saravan et al[5] studied on the active damping in a FRP composite cylindrical shell with skewed PVDF sensor/actuator. Suleman[6] proposed the finite element model for shell type adaptive composite finite element with electromechanical properties and with double curvature. Tzou et al[4] and Saravan et al[5] developed semi-analytical methods. Tzou et al[4], Saravan et al[5] and Suleman et al[6] performed numerical simulations for verification. In our recent paper 7, the active vibration control of isotropic shell structures using modal sensor/actuator systems was studied. In this paper, we extend these methods to design sensor/actuator system of the active vibration control of composite shell structures.

With this backgrounds, the distributed modal sensor/actuator system for the active vibration control of composite shell structure is designed. For the material of the sensor/actuator, PVDF film is used. Finite element method is adapted and developed to model the integrated structure, the shell structure with sensor/actuator system. The nine-node Mindlin shell element is used in finite element modeling of shell. To design modal transducer, the equation of motion is transformed into modal coordinate. A few of lowest modes, dominant in vibration, are considered in the design of sensor/actuator system. Sensor is designed to minimize the observation spillover, and actuator is designed to minimize the system energy in the control modes under given initial condition. The electrode pattern and the lamination angle of PVDF are optimized to satisfy these design objectives. Genetic algorithm is used as optimization scheme. LQG controller is designed for the control law. To demonstrate the feasibility of employing the designed system, the real time experiments of open and closed loop system of the integrated structure are performed after numerical optimization and simulation.

System Model

2.1. Finite Element Formulation

2.1.1 Mindlin Shell Element

Finite element method has been adopted in modeling the integrated structure of laminated composite shell with PVDF sensor/actuator. The nine-node Mindlin shell element8 with five nodal degrees of freedom composed of three translations and two rotations has been used. This element is able to account for transverse shear deformation. The adjacent nodes in the thickness direction are constrained to have the same displacement in the thickness direction.

From Figure 1 and Figure 2, the Cartesian Coordinates of an arbitrary point are described as Eq.(1).

$$\begin{Bmatrix} x \\ y \\ z \end{Bmatrix} = \sum N_i \begin{Bmatrix} x_i \\ y_i \\ z_i \end{Bmatrix} + \sum N_i (t_{0k} + \zeta \frac{t_k}{2}) \begin{Bmatrix} l_i \\ m_i \\ n_i \end{Bmatrix} \tag{1}$$

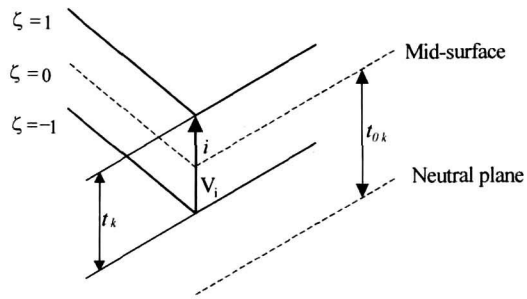

Fig. 1. Definition of the thickness and normal vector

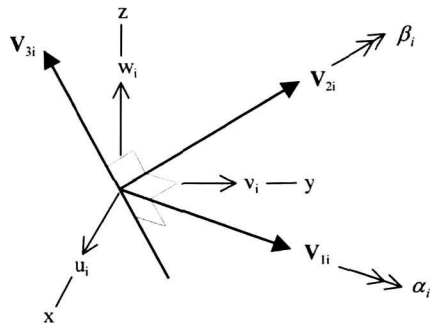

Fig. 2. Definition of directional cosine and nodal degree of freedom

t_k is the thickness of the k th layer, t_{0k} is the distance from midsurface of the k th layer from neutral plane of the structure. N_i is the shape function of the node i and is a function of ξ and η, not of ξ. l_{3i}, m_{3i} and n_{3i} are the components of the direction cosine vector $\mathbf{V}_{3i}$ of the line normal to the mid surface. $\mathbf{V}_{1i}$ and $\mathbf{V}_{2i}$ are tangent to the midsurface, perpendicular to each other and $\mathbf{V}_{3i}$ at the same time.

The displacement vector $\mathbf{v}$ and strain tensor $\boldsymbol{\varepsilon}$ are interpolated with nodal displacement by interpolation function, $\mathbf{N}$ and $\mathbf{B}$, respectively.

$$\mathbf{v} = \mathbf{NU}, \quad \boldsymbol{\varepsilon} = \mathbf{BU} \tag{2}$$

Made of orthotropic material, the composite shell structure has different material properties along the direction. $\overline{\mathbf{E}}$, the material property matrix defined on the material coordinate system, is transformed to the local coordinate system by applying the coordinate transformation matrix $\mathbf{T}_m$ which represents the lamination angle of orthotropic material.

$$\mathbf{E} = \mathbf{T}_m^T \overline{\mathbf{E}} \mathbf{T}_m \tag{3}$$

$\overline{\mathbf{B}}$, the strain-displacement relation matrix defined on the local coordinate system, is transformed to the global coordinate system by the geometric coordinate transformation matrix $\mathbf{T}_e$ as $\mathbf{B} = \mathbf{T}_e \overline{\mathbf{B}}$.

Then the element stiffness matrix and the element mass matrix are defined as Eq.(4).

$$\underset{5N\times 5N}{\mathbf{k}} = \int_{-1}^{1}\int_{-1}^{1}\int_{-1}^{1} \underset{5N\times 6}{\mathbf{B}}^T \underset{6\times 6}{\mathbf{E}} \underset{6\times 5N}{\mathbf{B}} \det \mathbf{J}\, d\xi\, d\eta\, d\zeta \tag{4-1}$$

$$\underset{5N\times 5N}{\mathbf{m}} = \int_{-1}^{1}\int_{-1}^{1}\int_{-1}^{1} \rho \underset{5N\times 3}{\mathbf{N}}^T \underset{3\times 5N}{\mathbf{N}} \det \mathbf{J}\, d\xi\, d\eta\, d\zeta \tag{4-2}$$

where ρ is mass density. The subscript N is the number of nodes in an element.

2.1.2 Piezoelectric Force Formulation

Considering the electric field only in the direction of thickness, the piezoelectric force vector $\mathbf{F}_p$ is formed as Eq.(5).

$$\mathbf{F}_P = \sum^{N_e} \left(\int \mathbf{B}_I^T \mathbf{e} \frac{1}{t_{PVDF}} dV_{PVDF} \right) \mathbf{S}_{PVDF} \tag{5}$$

t_{PVDF} is the thickness of PVDF film and V_{PVDF} is the volume of it. $\mathbf{B}_I$ is the inplane component of the strain-displacement relation matrix of PVDF film($\mathbf{B}_{PVDF}$). The electrode pattern vector $\mathbf{S}_{PVDF}$ is binary string vector whose components represent whether the electrode of each element is removed or not.

$$\mathbf{S}_{PVDF}(i) = \begin{cases} 1, & \text{if the electrode on } i\text{-th element } \textit{remains} \\ 0, & \text{if the electrode off } i\text{-th element is } \textit{removed} \end{cases} \tag{6}$$

The PVDF film is treated as an isotropic material, but electrically it is anisotropic. So, the performance of sensor/actuator systems is also varied by the lamination angle of PVDF. The piezoelectric constant vector $\mathbf{e}$ is transformed from material coordinate to global coordinate as Eq.(7).

$$\mathbf{e} = \mathbf{T}_{PVDF} \bar{\mathbf{e}} = \mathbf{T}_{PVDF} \mathbf{Cd} \tag{7}$$

$\mathbf{e}$ is piezoelectric stress constant vector in global coordinate system, $\bar{\mathbf{e}}$ is piezoelectric constant vector in material coordinate system and $\mathbf{T}_{PVDF}$ transformation matrix with the lamination angle on PVDF film. The piezoelectric stress constant vector $\bar{\mathbf{e}}$ is expressed with piezoelectric stiffness matrix $\mathbf{C}$ and piezoelectric strain constant vector $\mathbf{d}$. Changes of the lamination angle of PVDF film can vary the inplane piezoelectric constants. Even more, the shear component of piezoelectric constant can be produced, which does not exist when the lamination angle is 0.

2.2 Modal Transformation of Equation of Motion

For the efficient analysis of the characteristics of vibration, a few lowest modes, which have dominant effects on the characteristics of vibration, are considered. Using modal coordinate transformation as Eq(8), the equation of motion in modal coordinate can be written as Eq.(9).

$$\mathbf{u} = \mathbf{\Phi} \boldsymbol{\eta} \tag{8}$$

$$\ddot{\boldsymbol{\eta}} + \mathbf{c}\dot{\boldsymbol{\eta}} + \mathbf{\Lambda}\boldsymbol{\eta} = \mathbf{\Phi}^T \mathbf{F}_P V_a \tag{9}$$

$\mathbf{\Phi}$ is modal matrix containing eigenvectors, $\boldsymbol{\eta}$ is modal coordinate vector and $\mathbf{\Lambda}$ is diagonal matrix of eigenvalues. $\mathbf{c}$ is assumed modal damping matrix defined as $\mathbf{c} = diag(2\zeta_1\omega_1, \cdots, 2\zeta_n\omega_n)$ and $\mathbf{\Phi}^T \mathbf{F}_P$ is defined as modal actuating force per unit voltage. $\mathbf{\Phi}^T \mathbf{F}_P$ can be considered as the degree of contribution of total actuating force $\mathbf{F}_P$ to the specific modal characteristics. The PVDF transducer can be used both as actuator or sensor. If used as sensor, PVDF transducer produces the electric charge according to the strain field. When the PVDF actuator is used as a sensor, the induced charge is obtained as follows.

$$q = \mathbf{F}_P^T \mathbf{u} = \mathbf{F}_P^T \mathbf{\Phi} \boldsymbol{\eta} \tag{10}$$

In above equation, $\mathbf{F}_P^T \mathbf{\Phi}$ is defined as modal force of PVDF sensor. The modal force $\mathbf{F}_P^T \mathbf{\Phi}$ can be considered as the criterion of the performance to sense a specific mode.

According to characteristics of modal force mentioned above, the performances of distributed modal sensor/actuator are varied with adjusting the modal forces of sensor/actuator. The modal force of the sensor/actuator is varied with $\mathbf{F}_P$ which is determined by the electrode

pattern and lamination angle of PVDF film as prescribed above. Therefore the electrode pattern and lamination angle of PVDF film are optimized to satisfy the design objective.

Control System Design

As a control law the Linear Quadratic Gausian (LQG) is used. LQG is based on the linear quadratic regulator with full state variable feedback followed by Kalman filter. LQG design is suitable for complicated systems such as large-scale space structure.

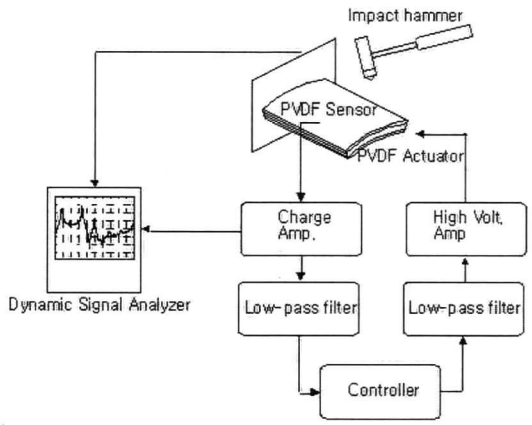

Fig. 3. System Setup for the closed loop control

Figure 3 is the brief configuration of the whole system. The output signal of sensor is presented as Eq.(11) if it has passed the charge amplifier, which has C_a as gain.

$$\mathbf{y}_{ca} = \frac{1}{C_a}\mathbf{F}_P^T \boldsymbol{\Phi}\boldsymbol{\eta} \tag{11}$$

Eq.(12) is the whole system matrix without controller. $\mathbf{x}_{fi}$ and $\mathbf{x}_{fo}$ are the low pass filter state variables, which are located at the input and the output of controller. $\mathbf{A}_f, \mathbf{B}_f, \mathbf{C}_f$ are state space matrices of the filter. $\mathbf{V}_a$ is control signal from controller, $\mathbf{y}$ is input signal to the controller. High voltage amplifier gain is K_a.

$$\dot{\mathbf{z}} = \begin{bmatrix} \dot{\boldsymbol{\eta}}_R \\ \ddot{\boldsymbol{\eta}}_R \\ \dot{\mathbf{x}}_{fi} \\ \dot{\mathbf{x}}_{fo} \end{bmatrix} = \begin{bmatrix} \mathbf{0} & \mathbf{I} & \mathbf{0} & \mathbf{0} \\ -\boldsymbol{\Lambda} & -\mathbf{C}_d & \mathbf{0} & \boldsymbol{\Phi}^T\mathbf{F}_{P\_ACT}\, K_a \mathbf{C}_f \\ \frac{1}{C_a}\mathbf{B}_f\mathbf{F}_{P\_SEN}^T\boldsymbol{\Phi} & \mathbf{0} & \mathbf{A}_f & \mathbf{0} \\ \mathbf{0} & \mathbf{0} & \mathbf{0} & \mathbf{A}_f \end{bmatrix} \mathbf{z} + \begin{bmatrix} 0 \\ 0 \\ 0 \\ \mathbf{B}_f \end{bmatrix} \mathbf{V}_a ,$$

$$y = [0 \quad 0 \quad \mathbf{C}_f \quad 0]\mathbf{z} \tag{12}$$

Separating the considered modal displacements ($\boldsymbol{\eta}_R$) into control modes ($\boldsymbol{\eta}_c$) and uncontrolled modes ($\boldsymbol{\eta}_u$) as Eq.(13).

$$\boldsymbol{\eta}_R = [\boldsymbol{\eta}_c \quad \boldsymbol{\eta}_u]^T \tag{13}$$

Substituting Eq.(13) into Eq.(12), Eq.(12) is rearranged as Eq.(14). The subscript c represents control mode while u denotes uncontrolled mode.

$$\dot{\mathbf{z}} = \begin{bmatrix} \dot{\boldsymbol{\eta}}_c & \ddot{\boldsymbol{\eta}}_c & \dot{\mathbf{x}}_{fi} & \dot{\mathbf{x}}_{fo} \end{bmatrix} = \mathbf{A}_c \mathbf{z}_c + \mathbf{B}_c \mathbf{V}_a \tag{14-1}$$

$$\dot{\mathbf{z}} = \begin{bmatrix} \dot{\boldsymbol{\eta}}_u & \ddot{\boldsymbol{\eta}}_u \end{bmatrix} = \mathbf{A}_u \mathbf{z}_u + \mathbf{B}_u \mathbf{V}_a \tag{14-2}$$

$$\mathbf{y} = \mathbf{C}_c \mathbf{z}_c + \mathbf{C}_u \mathbf{z}_u \tag{14-3}$$

Eq.(14) is converted to the discrete form as follows. $\boldsymbol{\Phi}_c(T_s)$ is discrete state transition matrix, and T_s is sampling time.

$$\mathbf{z}_c(k+1) = \boldsymbol{\Phi}_c(T_s)\mathbf{z}_c(k) + \boldsymbol{\Gamma}_c \mathbf{V}_a(k), \qquad \mathbf{y}(k) = \mathbf{C}_c \mathbf{z}_c(k) \tag{15}$$

Using the methods mentioned above, discrete LQG controller has been designed as Eq.(16). K_f is Kalman filter gain and K_c is the controller gain from LQR.

$$\bar{\mathbf{z}}_c(k+1) = \boldsymbol{\Phi}_c(T_s)\bar{\mathbf{z}}_c(k) + \boldsymbol{\Gamma}_c \mathbf{V}_a(k) + \boldsymbol{\Phi}_c(T_s) K_f (\mathbf{y}(k) - \mathbf{C}_c \bar{\mathbf{z}}_c(k)) \tag{16-1}$$

$$\mathbf{V}_a(k) = -K_c \bar{\mathbf{z}}_c(k) \tag{16-2}$$

In the design of LQR controller gain K_c, the weight matrix of the state variable $\mathbf{Q}$ and the weight matrix on control input $\mathbf{R}$ is selected as Eq.(17) respectively.

$$\mathbf{Q} = \mathbf{C}^T \mathbf{C}, \quad \mathbf{R} = \rho \mathbf{I} \tag{17}$$

In the design of Kalman filter gain K_f, the disturbance $\mathbf{W}$ and the measurement noise $\boldsymbol{\Theta}$ and disturbance displacement Γ are assumed as follow.

$$\mathbf{W} = q\mathbf{I}, \qquad \boldsymbol{\Theta} = \mathbf{I}, \quad \Gamma = \mathbf{B} \tag{18}$$

As q increases, the disturbance effect reduces. As ρ decreases, the designed controller will have larger control effect. Iterative method is adopted to choose the appropriate values of ρ and q.

Impact hammer is used to equally excite the whole modes of the system. Considering the external force from impact hammer ($\mathbf{F}_{EXT}$), the system matrix is defined as Eq.(19).

$$\begin{bmatrix} \dot{\eta} \\ \ddot{\eta} \end{bmatrix} = \begin{bmatrix} \mathbf{0} & \mathbf{I} \\ -\boldsymbol{\Lambda} & -\mathbf{C}_d \end{bmatrix} \begin{bmatrix} \eta \\ \dot{\eta} \end{bmatrix} + \begin{bmatrix} \mathbf{0} & \mathbf{0} \\ \boldsymbol{\Phi}^T \mathbf{F}_{P\_ACT} & \boldsymbol{\Phi}^T \mathbf{F}_{EXT} \end{bmatrix} \begin{bmatrix} \tilde{\mathbf{u}} \\ \mathbf{1} \end{bmatrix},$$
$$\bar{\mathbf{y}} = \frac{1}{C_a} \begin{bmatrix} \mathbf{F}_{P\_SEN}{}^T \boldsymbol{\Phi} & \mathbf{0} \end{bmatrix} \begin{bmatrix} \eta \\ \dot{\eta} \end{bmatrix} \tag{19}$$

Optimal Design of the Sensor/Actuator

4.1 Optimization Scheme

Genetic algorithm[10] is used for the optimization of electrode patterns and lamination angle of PVDF sensor and actuator. Optimization of electrode pattern, which determines whether an electrode segment of PVDF remains or is removed, is a discrete problem, thus genetic algorithm is suitable. The electrode is divided into many segments by the size of finite element. Unlike the electrode pattern, the lamination angle is not discrete value but continuous value. Therefore, to handle it using genetic algorithm, the continuous value of lamination angle between -90° and 90° is encoded into discrete value using 5-bit binary string. Table 1 shows the binary string representation of lamination angle. The number of design variables is equal to the sum of the number of elements used in the finite element method and five bits which represent the lamination

Table 1. Five-bit binary string representation of lamination angle of PVDF

Lamination Angle	Binary String	Lamination Angle	Binary String
-90°	00000	0 °	10000
-80 °	00001	5 °	10001
-70 °	00010	10 °	10010
-65 °	00011	.	.
.	.	.	.
.	.	.	.
.	.	80 °	11111

angle. In the optimization process with genetic algorithm, the probability of crossover is selected to be 0.3, the probability of mutation is chosen to be 0.06 and the population is set as 500.

4.2 Performance Index for the Design of Sensor/Actuator

A few lowest modes are considered in the design of sensor/actuator. The lower modes that have larger effects are chosen as control modes to be suppressed by active vibration control and the others are chosen as residual modes to be cut off to prevent the spillover.

4.2.1 Sensor Design Criteria

Sensor design is based on the idea of minimizing the observation spillover from the residual modes. So the signal from control modes is to be maximized and that of residual modes is to be minimized to prevent observation spillover. To satisfy this design objective, modal forces of residual modes are minimized, while those of control modes are maximized. Thus, the performance index to be maximized is set as follows.

$$J = \min(\left|\boldsymbol{\Phi}_c{}^T \mathbf{F}_P\right|) - \max(\left|\boldsymbol{\Phi}_u{}^T \mathbf{F}_P\right|) \tag{20}$$

$\boldsymbol{\Phi}_c{}^T \mathbf{F}_P$, $\boldsymbol{\Phi}_u{}^T \mathbf{F}_P$ are modal forces for the control modes and residual modes, respectively.

4.2.2 Actuator Design Criteria

For the actuator design, the energy in the closed loop system is used as a performance index, J as follows.

$$J = E(0) / \int_0^\infty (\dot{\boldsymbol{\eta}}_C^T \dot{\boldsymbol{\eta}}_C + \boldsymbol{\eta}_C^T \boldsymbol{\Lambda}_C \boldsymbol{\eta}_C^T + \rho u^2) dt \tag{21}$$

$E(0)$ is initial system energy, $\boldsymbol{\eta}_c$ is modal coordinate of control mode. ρ is the weighting for the control signal, which does not affect the actuator design and optimization result. Unlike sensor design, only the control modes are considered in actuator design.

The performance index, Eq.(21), is acquired by solving the LQR problem for system energy in control modes and changes with initial condition.

LQR problem for system energy is solved as follows.

Minimize

$$\tilde{J} = \frac{1}{2} \int_0^\infty \left(\begin{bmatrix} \boldsymbol{\eta}_c \\ \dot{\boldsymbol{\eta}}_c \end{bmatrix}^T \mathbf{Q} \begin{bmatrix} \boldsymbol{\eta}_c \\ \dot{\boldsymbol{\eta}}_c \end{bmatrix} + V_a \mathbf{R} V_a \right) dt \tag{22-1}$$

where

$$\begin{bmatrix} \dot{\boldsymbol{\eta}}_c \\ \ddot{\boldsymbol{\eta}}_c \end{bmatrix} = \begin{bmatrix} \mathbf{0} & \mathbf{I} \\ -\boldsymbol{\Lambda}_c & -\mathbf{C}_c \end{bmatrix} \begin{bmatrix} \boldsymbol{\eta}_c \\ \dot{\boldsymbol{\eta}}_c \end{bmatrix} + \begin{bmatrix} \mathbf{0} \\ \boldsymbol{\Phi}_c^T \mathbf{B}_a \end{bmatrix} V_a = \mathbf{A} \begin{bmatrix} \boldsymbol{\eta}_c \\ \dot{\boldsymbol{\eta}}_c \end{bmatrix} + \mathbf{B} V_a \tag{22-2}$$

$$\mathbf{Q} = \begin{bmatrix} \Lambda_c & \mathbf{0} \\ \mathbf{0} & \mathbf{I} \end{bmatrix}, \quad \mathbf{R} = \rho \mathbf{I} \tag{22-3}$$

The minimum of $\tilde{J}$ is determined with the initial state variables as follows.

$$\tilde{J}_{\min} = \frac{1}{2}\begin{bmatrix} \boldsymbol{\eta}_c^0 \\ \dot{\boldsymbol{\eta}}_c^0 \end{bmatrix}^T \mathbf{P} \begin{bmatrix} \boldsymbol{\eta}_c^0 \\ \dot{\boldsymbol{\eta}}_c^0 \end{bmatrix} \tag{23}$$

$\mathbf{P}$ is the solution of the Riccatti Equation shown in Eq.(24).

$$\mathbf{A}^T\mathbf{P} + \mathbf{PA} + \mathbf{Q} - \mathbf{P}^T\mathbf{BR}^{-1}\mathbf{B}^T\mathbf{P} = \mathbf{0} \tag{24}$$

then the performance index is rewritten as

$$J_{actuator} = \left[\sum_{\text{k=control modes}} E_0^k \right] / \tilde{J}_{\min} \tag{25}$$

E_0^k is the initial energy of the k-th mode. The activation force of the specific mode can be changed with the variation of the initial energy ratio. Consider the potential energy of the initial energy only, the initial state variable of the k-th mode η_0^k is determined from the initial energy as

$$\eta_0^k = \sqrt{E_0^k} \Big/ \varpi_k \tag{26}$$

ϖ_k is the natural frequency of the k-th mode.

Optimized Design results

To verify the methods mentioned above, the single curved cantilevered composite shell structure is used as host structure in the design of sensor/actuator system. Figure 4 shows the configuration of integrated structure of 1/9 cylindrical shell with one end clamped. Carbon/epoxy prepreg is used for the material of host structure and PVDF film is used for the sensor and actuator. The PVDF films are laminated in both sides of the host structure. The one over the host structure is selected as a sensor, the other one is set to be an actuator. The material properties of Carbon/epoxy prepreg and PVDF are shown in Table 2. The thickness of PVDF film is 52mm. The thickness of a sheet of Carbon/epoxy prepreg is 0.122mm. $[45]_{2s}$ laminated composite shell is used for the host structure.

Table 2. Material Properties of Carbon/Epoxy prepeg and PVDF film

PVDF film	Carbon/Epoxy prepreg
E = 3.0 GPa ν = 0.33 ρ = 1780 kg/m^3 d_{31} = 23e-12 v/m d_{32} = 3e-12 v/m	E_{11} = 137.85 GPa E_{22} = 9.83 GPa G_{12} = 5.6 GPa G_{13} = 5.6 GPa G_{23} = 2.8 GPa ν_{12} = 0.295 ρ = 1532 kg/m^3

Table 3. Natural frequencies of integrated structure

Mode	1st	2nd	3rd	4th	5th
Frequency(Hz)	99.7	185.6	319.4	425.9	445.3

The five lowest modes are included in the analysis. The lowest two modes are selected for the control modes and the other three are selected for residual modes. The natural frequencies derived from modal reduction are appeared in Table 3.

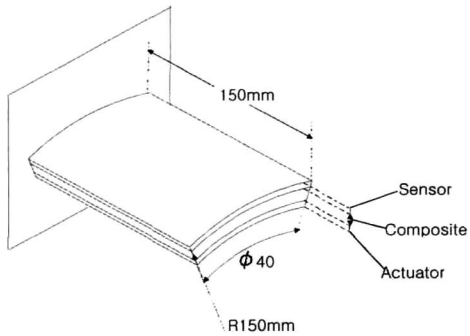

Fig. 4. Configuration of Specimen

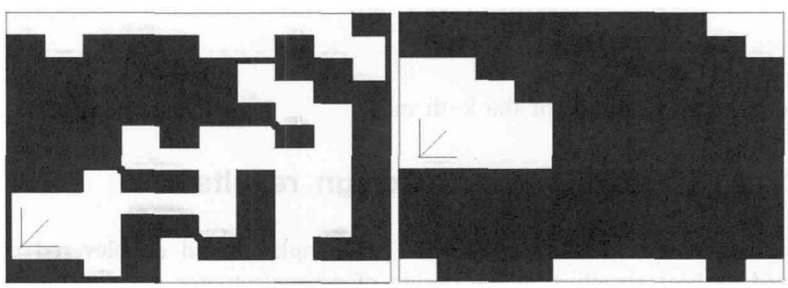

(a) Sensor electrode pattern (0°) (b) Actuator electrode pattern (0°)

Fig. 5. Optimized electrode pattern and lamination angle of sensor and actuator

Table 4. Modal forces per unit voltage of the optimized sensor/actuator

Mode	Sensor	Actuator
1st	4.272398e-04	-5.533933e-04
2nd	-5.472428e-04	9.397839e-04
3rd	1.780752e-07	9.041878e-04
4th	-3.447899e-07	1.766863e-04
5th	6.252322e-07	5.111947e-04

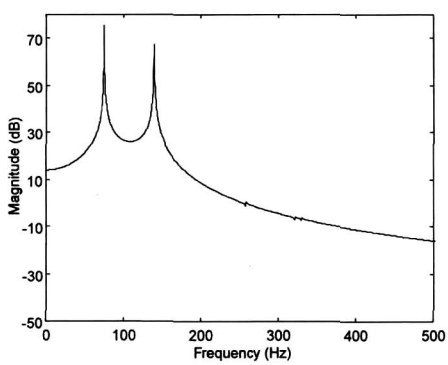

Fig. 6. Transfer function of optimized sensor - (Simulation)

The electrode patterns and lamination angles of the sensor/actuator are optimized as Figure 5. Due to the restriction in manufacturing, the lamination angles of the sensor and actuator are confined to 0. The modal forces of the optimized sensor and actuator are shown in Table 4. The modal forces of the residual modes are dramatically reduced to as small as 1/1000 of those of the control modes. As the distribution of the modal forces shown in Table 4, the transfer function of optimized sensor in Figure 6 delineates that the signal of the residual modes is diminished.

Experiments

System for the closed loop system is setup as illustrated in Figure 3. The parameters used in the system are sampling frequency of 5kHz, charge amplifier gain of 108 V/F, the high voltage amplifier gain of 100V/V and the cutoff frequency of 205Hz. To confine the input voltage to the PVDF film actuator within 400 V, the control signal from the controller is limited within 4 V.

Figure 7 shows the specimen with PVDF sensor and actuator covered. The white one is PVDF film with its electrode on, while black one is the composite shown thorough the PVDF film where its electrode has been removed.

Figure 8 is the transfer function of the optimized sensor and actuator obtained by the experiment. The transfer function clearly manifests that signals from the residual modes are reduced compared with those of control modes. The transfer function of optimized actuator shows that the optimized actuator excites the first and second modes effectively. In the design of LQG controller, the empirical natural frequencies of the control modes are used in determination of the weighting factors. The weighting factors of disturbance and control input are 0.05 and 12000, respectively. These factors have been determined empirically.

The comparison of the transfer functions of open and closed loop is described in Figure 9. Compared with the open loop transfer function, the magnitudes of the first and the second modes

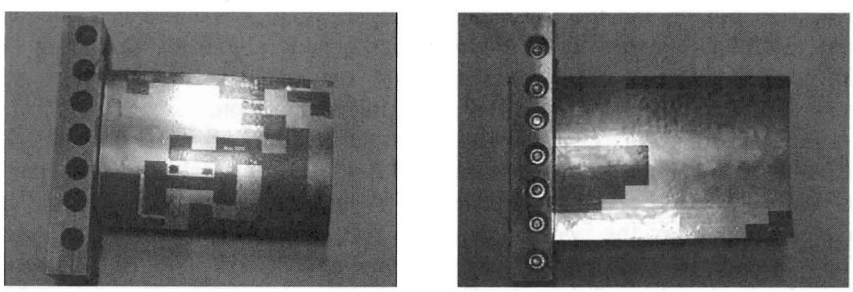

(a) Specimen with Sensor side up (b) Specimen with Actuator side up

Fig. 7. Specimen covered with PVDF sensor / actuator

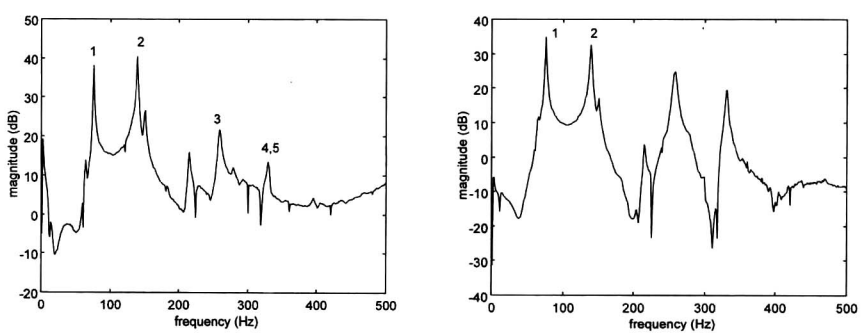

(a) Sensor transfer function (b) Actuator transfer function

Fig. 8. Transfer function of optimized sensor and actuator (Experiment)

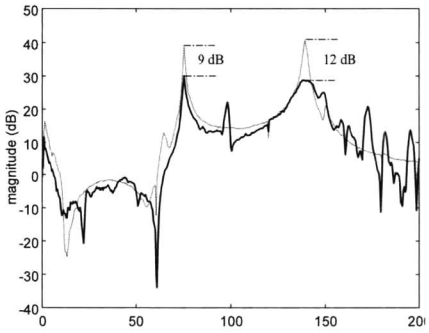

Fig. 9. Comparison of Open and Closed loop transfer functions

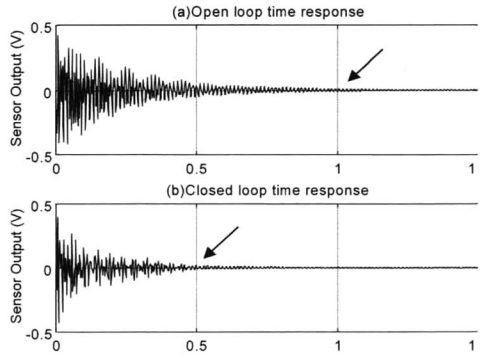

Fig. 10. Open and closed loop time responses (Experiment)

of the closed loop are reduced by 9 dB and 12dB, respectively. Figure 10, the time responses of open and closed loop systems, shows that the settling time of the closed loop has been reduced to approximately 50% compared with that of open loop system.

Conclusion

In this paper, the modal sensor/actuator system is optimized to control the vibration of composite shell structure. Sensor/actuator system is made of PVDF film. The nine-node Mindlin shell element is used in the finite element modeling of the integrated structure which is composed of a composite shell structure with PVDF sensor/actuator.

The electrode pattern and the lamination angle of PVDF are discretized into binary string and optimized to satisfy the design objectives using genetic algorithm. Sensor is optimized to minimize the adverse effect of observation spillover, and actuator is designed to minimize the system energy of the control modes under a given initial condition.

Active vibration control experiments have been successfully accomplished with the designed results. Discrete LQG controller is used as a control law. Experimental results of open and closed loop system demonstrate the good performances of designed modal sensor/actuator system. The residual mode signals from the sensor were cut off and the spillover phenomenon did not occurred. The vibrations of the control modes, first and second modes, are suppressed by 9dB and 12dB, respectively. In the view of time domain, the settling time of the closed loop have reduced to approximately 50% of that of the open loop.

ACKNOWLEDGEMENT

The research was supported in part by a grant from the BK-21 Program for Mechanical and Aerospace Engineering Research at Seoul National University.

REFERENCES

1. Balas, M.J., "Feedback Control of Flexible Systems", IEEE Transactions on Automatic Control, AC-23, No. 4, pp. 673-679, 1978.

2. Balas, M.J., "Feedback Control of Flexible Systems", IEEE Transactions on Automatic Control, AC-23, No. 4, pp. 673-679, 1978.

3. Meirovitch, L. and Baruh, H., "The Implementation of Modal Filters for Control of Structures", Journal of Guidance and Control, 8, No.6, pp.707-716, 1985.

4. S.J. Kim, J.S. Hwang, J. Kim, "System design of distributed modal transducer by adjustingspatial gain distribution", SPIE's 6th International Symposium on Smart Structures and Materials, Newport Beach, California, U.S.A., March 2, 1999.

5. Zhou,Y. and Tzou, H.S., "Active control of nonlinear piezoelectric circular shallow spherical shells", International Journal of Solids and Structures, 37, pp.1663-1677, 2000.

6. Saravan, C., Genesan N. and Ramamurti, V., " Analysis of active damping in composite laminate cylindrical shells of revolution with skewed PVDF sensor/actuators", Composite Structures, 48, pp. 305-318, 2000.

7. Suleman, A., "Adaptive composite modelling and application in panel flutter and noise suppression", Computers and Structures, 76, pp.365-378, 2000.

8. S.J. Kim, J.S. Hwang, J.W. Mok, "Sensor/Actuator Design for Active VibrasionSystem design of distributed modal transducer by adjusting spatial gain distribution", SPIE's 7th International Symposium on Smart Structures and Materials, Newport Beach, California, U.S.A., March 2, 1999.

9. Cook, R.D., Malkus, D.S. and Plesha, M.E., Concepts and application of finite element analysis, John wiley & Sons, New York, 1989.

10. Lee, C.K., "Theory of laminated piezoelectric plates for the design of distributed sensors/actuators: part I: Governing equations and reciprocal relationships", Journal of Acoustic Society of America, 87, No. 3, pp. 1144-1158.